FINAL TECHNICAL REPORT

3D Structural Velocity (Vp) Model of the Ventura Basin, California, for Improved Strong Ground Motion Prediction

by:

John H. Shaw, Charles M. Brankman, and Andreas Plesch

Department of Earth and Planetary Sciences

Harvard University

20 Oxford Street, Cambridge, MA 02138

phone: 617-495-0367

fax: 617-495-7660

email: shaw@eps.harvard.edu

U.S. Geological Survey

National Earthquake Hazard Reduction Program

Award No. 08HQGR0025

March 31, 2009

Research supported by the U.S. Geological Survey (USGS), Department of the Interior, under USGS award number 08HQGR0025. The views and conclusions contained in this document are those of the authors and should not be interpreted as necessarily representing the official policies, either expressed or implied, of the U.S. Government.

Abstract

The Ventura Basin is a tectonically active basin in southern California that contains a thick Cenozoic sedimentary sequence. To assess the effect of these sediments and the basin structure on coseismic ground motions, we integrate an extensive dataset of petroleum industry geophysical data with published geologic maps and structural cross sections into a three-dimensional structural and velocity model of the basin. The top Cretaceous surface is considered the base of the sedimentary section, and represents the transition between low velocity Cenozoic sediments with the higher velocity basement. This surface is mapped across the basin and incorporates displacements across the major basin bounding faults. The P-wave velocity structure of the sediments is investigated using sonic logs and stacking velocities from seismic reflection data. The velocity gradient of the basin can be described as a simple power law function of depth. This relationship is used to populate a three-dimensional velocity model of the basin, which is then used to characterize ground motions associated with four historical earthquakes using empirical attenuation relationships for southern California. The results clearly show the effect of basin structure on amplified ground motions for all cases. The velocity model will be used in future numerical wave propagation simulations to assess the impact of basin resonance and rupture directivity on ground motions in the basin.

Introduction

Ground motions associated with large earthquakes are greatly affected by the characteristics of the earth materials through which the coseismic waves pass. Low seismic velocities associated with geologically young, unconsolidated and semi-consolidated sedimentary units cause amplification of seismic waves, increasing ground motions and associated seismic hazards. In addition, sedimentary basin structure can cause basin resonance, prolonging the duration of shaking during a seismic event. For these reasons, the characterization of the structure of sedimentary basins in seismically active regions is crucial for the accurate understanding of earthquake ground motion related hazards.

The Ventura Basin (Figure 1) is located in the Transverse Ranges province of southern California, and is a deep, geologically young, tectonically active sedimentary basin in a region of high earthquake hazard. The basin is bounded on its northern and southern margins by active reverse and oblique reverse faults, and also has several active faults and folds within the basin. The basin contains the thickest Plio-Pleistocene sedimentary section in the world (Yeats, 1977; Yeats et al., 1988). Active basin subsidence and uplift of the bounding basement blocks has resulted in the deposition of up to 15 km of Cenozoic sediments. The basin comprises a major petroleum province, and has been the focus of extensive oil exploration for over a century. Despite the abundance of subsurface data from oil exploration wells and geophysical surveys, however, a detailed regional understanding of the velocity structure of the basin is lacking.

In this NEHRP sponsored research effort, we developed a three-dimensional velocity model of the Ventura Basin that was derived from subsurface data from the petroleum industry. We integrate direct velocity measurements from sonic logs of 60 petroleum wells with stacking velocities from a regional seismic reflection survey to develop a velocity model for the Cenozoic sedimentary section in the basin. This model is applied to a new structural model of the basin that was generated from published maps and cross sections. Using empirical attenuation relationships of earthquake ground motions, we show examples of several historic and scenario earthquakes that highlight the effect of basin structure on ground motions. These models provide a framework for future detailed models of coseismic wave propagation and ground motion prediction in the Ventura Basin that will contribute to the assessment and mitigation of earthquake hazards in the area.

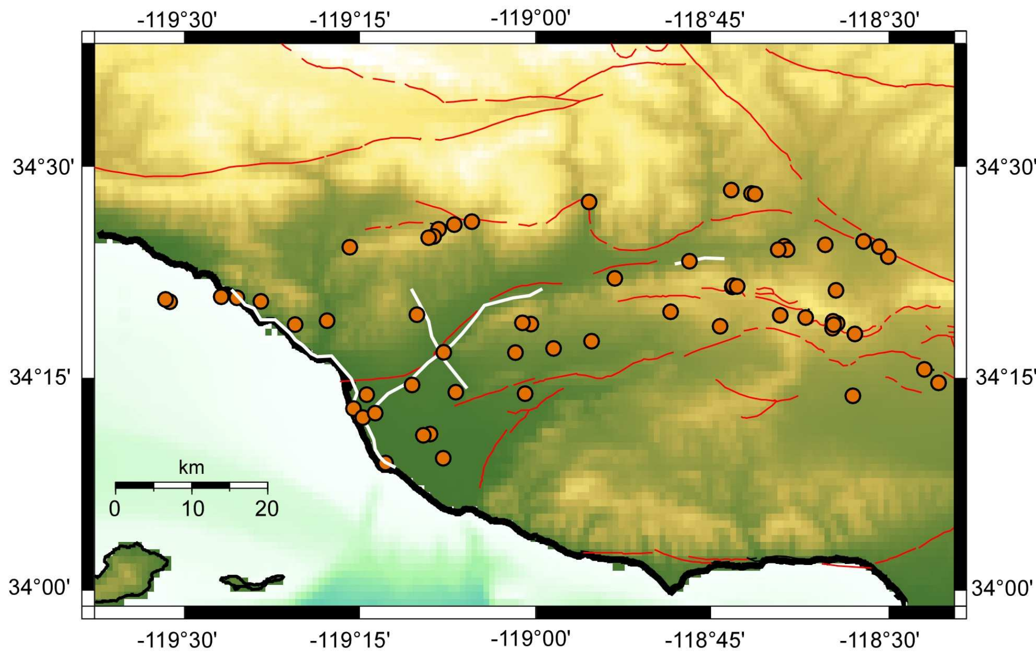

Figure 1 – Regional location map of the Ventura basin, showing wells (orange) and seismic lines (white) used in the study. Active faults (Jennings, 1994) are shown in red.

Regional Geology and Basin Structure

The Ventura basin lies in the Transverse Ranges province of southern California (Reed and Hollister, 1936; Vedder et al., 1969), an east-west trending fold-and-thrust belt that developed from the Pliocene through the Quaternary (Yeats, 1983; Namson and Davis, 1988a; Shaw and Suppe, 1994). Recent studies of folding and faulting (e.g., Namson and Davis, 1988a; Yeats et al., 1988; Yeats 1983, 1988; Yeats and Huftile, 1995; Huftile and Yeats, 1995; Shaw and Suppe, 1994; Kamerling et al., 2001; Pinter, 2003) and present-day stress measurements (Mount and Suppe, 1992) indicate that regional contraction and compression are directed north-south to northeast-southwest, roughly normal to the San Andreas fault (Zoback et al., 1987; Hauksson, 1990). Shortening on faults and folds in this tectonic province accommodates a component of the discrepancy between the estimated relative Pacific-North American plate motion and observed slip on the San Andreas fault (Minster and Jordan, 1978; Demets et al., 1987). Pliocene and Quaternary folding (Jackson and Yeats, 1982; Namson and Davis, 1988a; Yeats et al., 1988; Yeats 1983, 1988; Yeats and Huftile, 1995; Yeats et al., 1994, Huftile and Yeats, 1995; Shaw and Suppe, 1994; Kamerling et al., 2001; Pinter, 2003) and Global Positioning System (GPS) studies (Larson and Webb, 1992; Larsen et al., 1993; Donnellan et al., 1993; Hager et al., 1999; Argus et al., 2000) have indicated from 5 to 15 millimeters per year of northeast-southwest shortening across the Ventura basin, which represents some of the fastest shortening rates in all of southern California. Several historic events, including the 1978 Ml = 5.1 Santa Barbara earthquake (Corbett and Johnson, 1982), and the 1994 M = 6.7 Northridge earthquake (U.S.G.S and S.C.E.C. Scientists, 1994), which occurred in the adjacent San Fernando basin east of the Ventura basin, indicate that a component of this shortening is being accommodated seismically.

Basin Model

Structural geology of the basin and basin margins

The structure of sedimentary basins has a primary effect on the distribution and magnitude of strong ground motions that result from large earthquakes, and thus has an important impact on regional seismic hazard. The Ventura basin is extremely deep, with total sediment thicknesses locally exceeding 10 km. Moreover, the basin is elongated in an east-west direction, with locally steep northern and southern borders that are formed by displacements on large blind-thrust and reverse faults and associated folds. These structures include the Oak Ridge, Ventura, San Cayetano, and Red Mountain faults, all of which are active and capable of generating large earthquakes. Many of these structures extend into the sedimentary basins, locally thrusting higher velocity basement rocks over lower velocity sediments. Similar velocity inversions in the Santa Monica region of the Los Angeles basin have been shown to have focused and amplified seismic waves during the 1994 Northridge (M 6.7) earthquake (e.g., Graves et al., 1998). Thus, characterizing the structure of the Ventura basin is of primary importance in the accurate assessment of the distributions of hazardous ground shaking that will result from large earthquakes on faults surrounding the basin, as well as other significant earthquakes on more distant sources such as the San Andreas Fault.

The subsurface structure of the Ventura basin has been studied in detail by various authors (e.g., Namson and Davis, 1988a; Yeats et al., 1988; Yeats, 1983, 1988; Yeats and Huftile, 1995; Yeats et al., 1994, Huftile and Yeats, 1995; Kamerling et al., 2001). In order to develop a comprehensive structural model of the Ventura basin, we integrated the results of these previous studies into a common digital model with additional seismic reflection and well bore data. These new and existing constraints were used to construct a three-dimensional structural model of the basin that includes the basin shape, realistic geometries and displacements on the bounding and internal faults.

In order to properly describe the size and shape of the basin in the new models, we incorporated topographic/bathymetric and geologic surfaces that are used to specify property boundaries. We used topography and bathymetry derived from GTOPO30, a global digital elevation model provided by the U.S. Geological Survey.

The primary stratigraphic surface that forms the lower boundary of the basin model is the top basement surface, which throughout much of the basin is represented by the top Cretaceous horizon. This surface was chosen because it represents a well defined contrast in lithology between the relatively less consolidated Cenozoic sediments and the underlying well indurated sediments and crystalline basement. The top Cretaceous surface has also been defined in several published maps and cross sections, while constraints on the top of crystalline basement are less well defined. Finally, the velocity contrast between the Cretaceous sediments and the underlying crystalline basement is probably relatively small, making the top Cretaceous more important for the velocity model. The top Cretaceous surface was constructed by integrating published maps and cross sections, as well as subsurface data from petroleum exploration wells. The surface is well imaged in seismic reflection data in the eastern Santa Barbara basin west of the Ventura basin, and the combination of well and seismic data places effective constraints on these surfaces throughout the Ventura basin.

All of the published data, the well logs, and the seismic data were georeferenced and integrated in Gocad (Mallet, 1992), a 3-D geologic CAD tool designed for the construction of surfaces, the analysis of spatially distributed data, and the modeling or simulation of properties. The structural constraints were used to interpolate triangulated surfaces that define the basin structure. Because faults form primary boundaries of the basin, the geologic horizons were constructed to be compatible with the locations and displacements of major faults. In this analysis, we used representations of the major fault systems represented in the SCEC Community Fault Model (CFM v 2.5) (Plesch et al., 2006).

The Ventura Basin is bounded on both the north and south by Holocene- and Quaternary-active reverse and oblique reverse faults. Using the fault representations and the surface constraints, we represent displacements of the top-basement surface across the large thrust faults that bound the basin, including the Oak Ridge, San Cayetano, and Red Mountain, and Santa Susana structures. These fault offsets have an important influence on the basement shapes, in particular by creating steep basin edges and local velocity inversions where high-velocity basement rocks are thrust over lower velocity sediments. The Red Mountain, San Cayatano, and Santa Susana faults are large north dipping, south vergent reverse faults that together form the northern margin to the central axis of the Ventura Basin. The top basement surface is offset by up to 10 km of reverse displacement on the San Cayatano Fault, with displacement transferred east onto the Santa Susana Fault and west onto the Red Mountain fault. The southern margin of the basin is bounded by the south dipping, north vergent Oak Ridge fault, which offsets the top basement surface by up to about 9 km of reverse displacement. These large displacements have resulted in large regions of the lower Cenozoic sedimentary section in the central basin to be overthrusted by hanging wall basement blocks, with resulting velocity inversions along the northern margin of the basin.

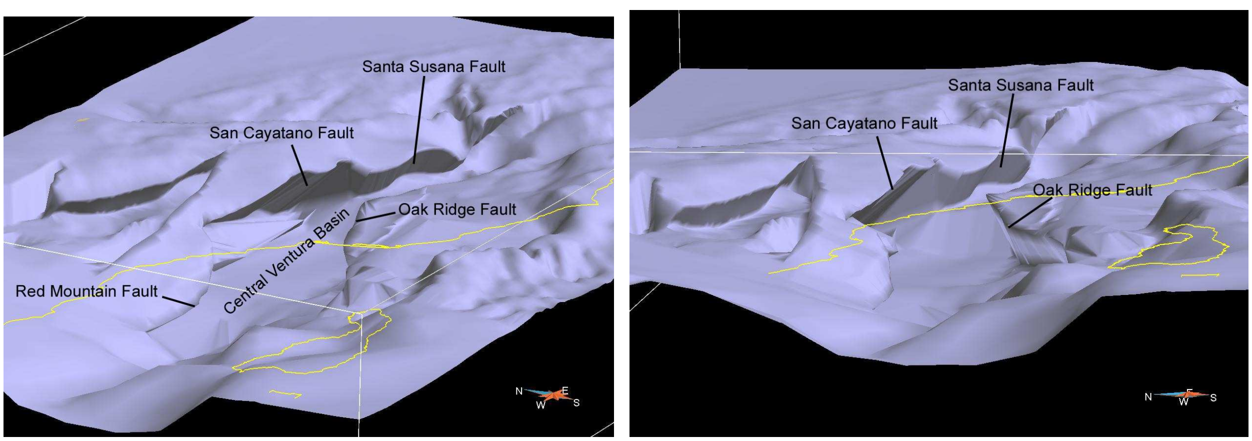

Figure 2. Perspective views of the composite basement surface of the Ventura basin model.

Basin P Wave Velocity Characterization

Sonic Logs

Direct measurements of the velocity structure of the Cenozoic basin fill are available in the form of sonic logs collected from petroleum exploration wells. Sonic logs are collected by measuring the interval transit time (ITT) between a source and receiver located on a logging tool that is moved continuously along a borehole. The source emits a signal, and the receiver records the P wave arrival. The spacing between the source and receiver is relatively small (1-2 m), so the measurements sample the sediments at a resolution of 0.5 – 1.0 m. The ITT measurements are then converted to P wave velocities that represent the in situ velocities of the sediments. P wave velocities are used in the petroleum industry to estimate reservoir parameters such as lithology, porosity, and density. Sonic log data have been used to characterize the velocity structure of other basins in southern California, including the Los Angeles basin (Süss and Shaw, 2003) and the Salton Trough (Lovely et al., 2006).

Sonic logs from 60 wells distributed throughout the Ventura basin and adjacent eastern Santa Barbara Channel (Figure 1) were collected and digitized. The sonic logs sample sediments ranging from the Quaternary to the Eocene in age, at depths from the surface to more than 5000 meters. The sonic logs from individual wells sample depths ranging from only a few hundred meters to more than 5000 m. A compilation of velocity measurements from throughout the basin shows a general pattern of linearly increasing P wave velocity with depth (Figure 3). This is a common relationship that is found in many sedimentary basins.

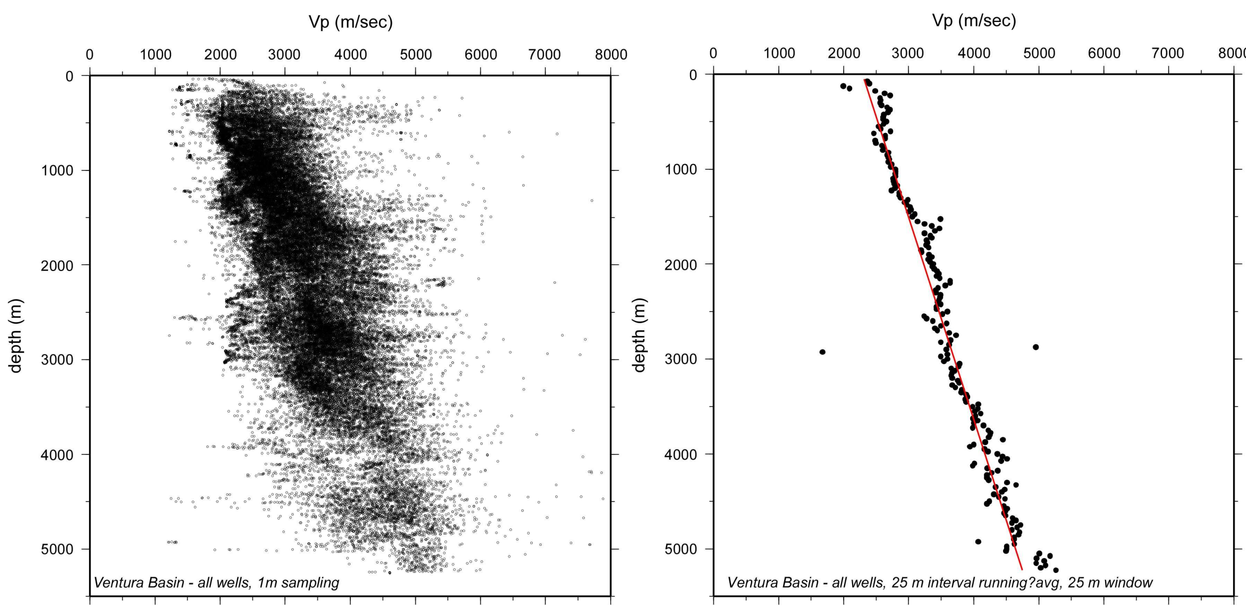

Figure 3. P wave velocity measurements from sonic logs of 60 wells in the Ventura Basin, taken at 1 m (left) and 25 m (right) samplings.

Seismic Stacking Velocities

In addition to the direct P wave velocity measurements from the sonic log data, we utilized stacking velocities derived from a seismic reflection survey collected across the basin. Stacking velocities are derived during the processing of seismic reflection data, and represent estimates of the averaged velocities above user-defined reflections. Individual layer velocities can then be calculated from the averaged velocities; these velocities represent the average P wave velocities of the individual layers. The scale of measurement of the stacking velocities is much greater than that of the sonic logs, and the velocity profiles derived from the stacking velocities results in step functions of velocity with depth. In order to compare the stacking velocity data with the sonic log data, we linearly interpolated the interval velocities taken from the stacking velocity data, and resampled them at the same interval as the sonic log data.

Stacking velocities from three 2-D seismic reflection lines were available for this study. One line extends roughly E-W along the axis of the basin, while the other two lines extend roughly N-S across the basin. A total of 699 interval velocities were computed from the stacking velocities of the three lines. The measurements sample depths from the ground surface to 7500 m, with interval velocities ranging from 1600 – 5500 m/sec (Figure 4).

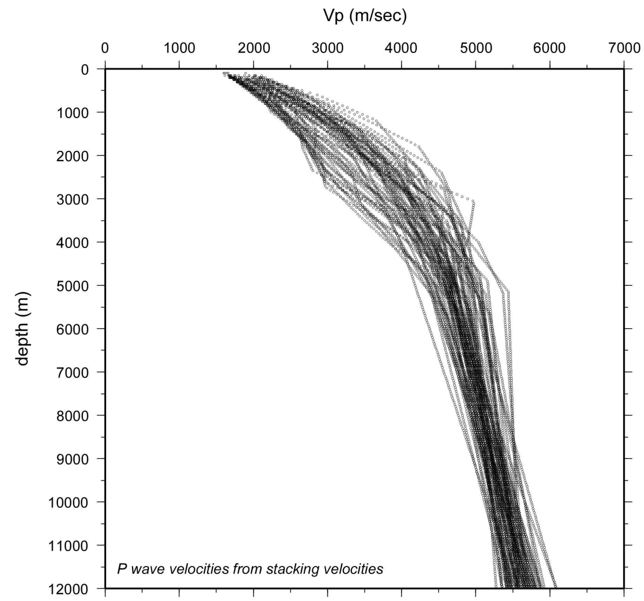

Figure 4. P wave velocity measurements derived from stacking velocities from seismic reflection lines in the Ventura Basin. Interval velocities were linearly interpolated and sampled at 50 m intervals.

Correlation of Stacking and Sonic Log Data

Because of the inherent differences in resolution of the two data sets, it is appropriate to compare the velocities derived from the sonic log data with those from the seismic stacking velocities. To do this, we compared sonic logs with stacking velocity measurements within a radius of 2 km from the well. Examples of these comparisons are given in Figure 5. In general, the stacking velocities correlate well with the more detailed sonic log measurements. There was a substantial mismatch between the two data sets for one well; however, because the sonic log for this well only sampled 350 m of the well, we could not confirm if this interval was representative of the entire borehole or was a local low velocity zone, perhaps due to the presence of a gas-bearing interval. Thus, the sonic log data from that well was removed from the data set and not used in the subsequent velocity analysis.

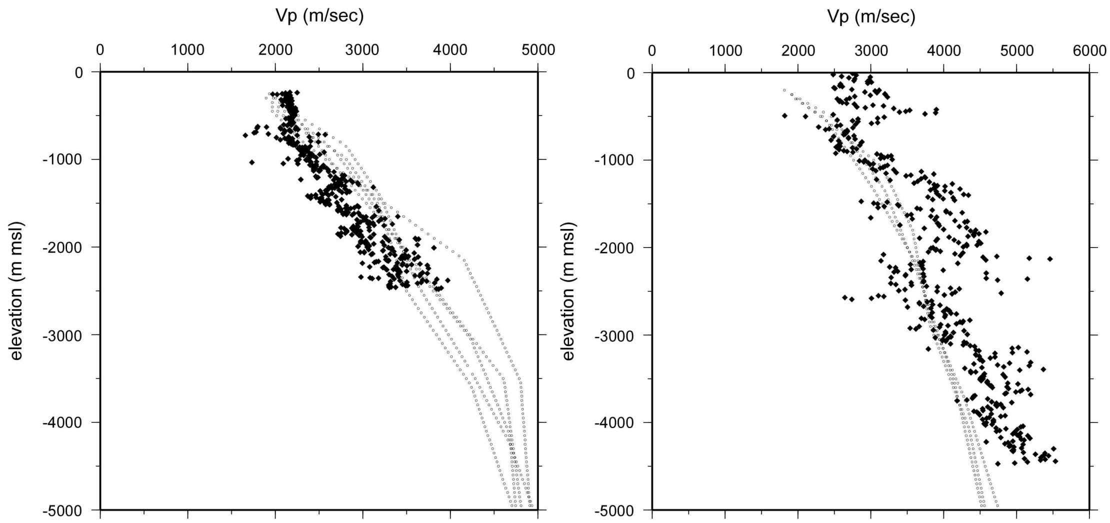

Figure 5. Comparisons of P wave velocities derived from sonic logs (black diamonds) and stacking velocity measurements within 2 km (gray circles). In general, the two datasets are well correlated throughout the basin.

Velocity Parameterization

A compilation of P wave velocities from the sonic log data and the interpolated stacking velocities shows good agreement between the two datasets (Figure 6). A general pattern of increasing P wave velocity with depth is observed, with the linearly increasing trend of the well data overlying the shallow stacking velocity data. The deeper stacking data, however, define a steeper velocity gradient, with P wave velocities increasing more slowly with depth than at shallower depths. The velocity gradient can be described by:

$$v_p = 361d^{0.2944}$$

where v_p is the P wave velocity in m/s, and d is the depth in m. This fit has an R^2 value of 0.9287, indicating that the fit of the data to this equation is robust.

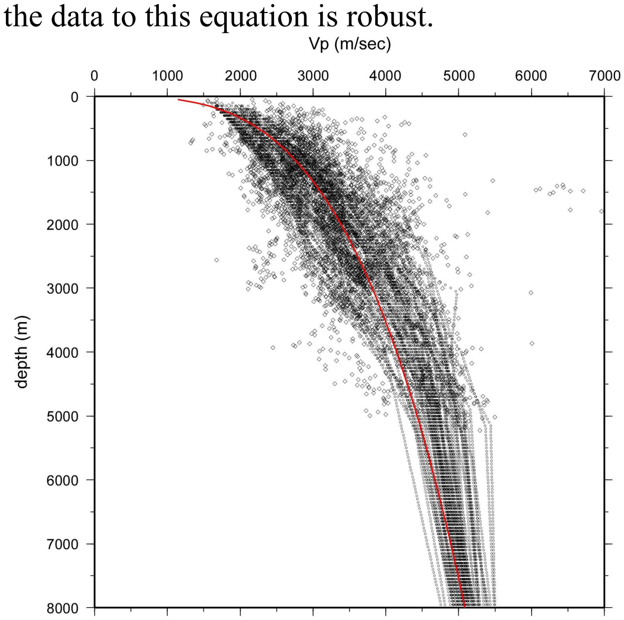

Figure 6. Compilation of P wave velocity measurements from sonic logs and stacking velocities in the Ventura basin. The best fit curve to the data is shown in red.

The equation relating P wave velocity to depth was used to populate a basin velocity model. Because the velocities are considered to vary with depth, the variations observed in the velocities at various depths are correlated with surface topographic features. However, the geometry of the basin margins, as defined by the bounding reverse faults, controls the spatial extent of the basin sediments. The variable extent of the sedimentary section is evident in the slices through the velocity model given in Figure 7.

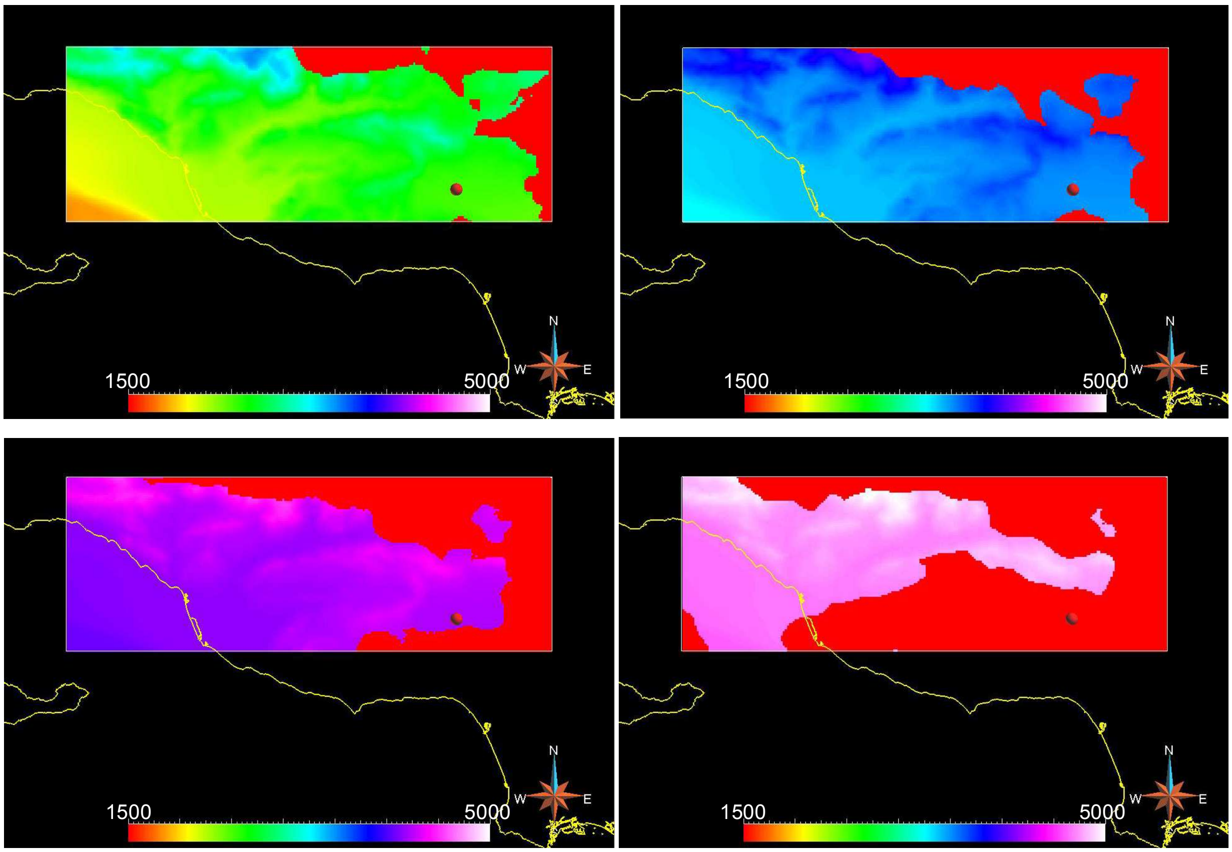

Figure 7. Horizontal slices through the P wave velocity model of the Ventura basin at a) -500 m, b) -2000 m, c) -4000m, and d) -6000m. Red areas represent regions of high velocity basement rock that were not included in the P-wave velocity model.

Effect of Basin Structure on Coseismic Ground Motions

In order to demonstrate the effect of the three dimensional structure of the Ventura basin on coseismic ground motions, we used our structural model as input to empirical ground motion calculations for several scenario and historic earthquakes. We utilized the empirical attenuation relationship developed by Field (2000) for southern California earthquake ground motions, which is described by:

$$\mu(M, r_{jb}, v_s) = b_1 + b_2(M\text{-}6) + b_3(M\text{-}6)^2 + b_5 ln[(r_{jb}^2 + h^2)^{0.5}] + b_v ln(v_s/v_a) + (6.7 \text{ x } 10^{-5})d - 0.14$$

for cases such as ours where the basin depth is known. In this equation, $\mu = ln(\text{PGA})$, M is moment magnitude, r_{jb} is the distance (km) to the vertical projection of the earthquake rupture, v_s is the average shear wave velocity (m/sec) of the upper 30 m of sediment, d is the basin depth (m), and v_a = 760 m/sec. Values for v_s were taken from a compilation map of the 30 m average shear wave velocity in Wells (2000). The other parameters (b_1, b_2, b_3, b_5, and h) are constrained by regression analysis, and were provided by Field (2000) for basins in southern California.

Four historic earthquakes were chosen to demonstrate the effect of the basin structure on the magnitude and distribution of coseismic ground motions. Figure 8 shows the results of surface PGA calculations for the 1857 Ft. Tejon (Figure 8a), the 1994 Northridge (8b), 1973 Pt. Mugu (8c), and 1978 Santa Barbara (8d) earthquakes. In general, the effect of the deep central basin is to amplify and focus the ground motions. Abrupt and dramatic variations in ground motion occur across the surface projections of the faults that bound the central basin.

The Ft. Tejon earthquake (M.7.9) occurred on the San Andreas fault about 30 km northeast of the basin. This scenario results in PGA values of up to 0.15g on the northern and southern basin margins, while the east-central basin experiences up to 0.31g. The contrast is greatest across the San Cayatano Fault on the northern margin of the basin; this is due to both the proximity to the earthquake source and the contrast in sediment depth across the fault. Ground motions of up to 0.21g extend west to the coast in the central basin, while ground motions on the margins decrease to 0.16g (north) and 0.10g (south).

The Northridge earthquake (M.6.7) occurred about 25 km southeast of the eastern Ventura basin. Ground motions are greatest in the immediate source area, and decrease to the west along the axis of the basin. The results for this case clearly show the effect of the deep central basin in allowing the propagation of the ground motions further along the basin axis than along the adjacent basin margins to the north and south. Accelerograms at the Santa Susana ETEC building site, located 16 km west of the epicenter, recorded coseismic ground motions of 0.29g during the Northridge earthquake (Porcella et al., 1994; Ventura et al., 1995). The results of the simulation using the velocity model developed here indicate a PGA of 0.26g, which is within 10% of the recorded ground motion. While a comprehensive verification of the velocity model cannot be done based on this one site alone, the results from this site indicates that the developed velocity model captures the first order effect of basin structure and sediment depth on coseismic ground motions.

The two other scenario earthquakes highlight the effect that the basin structure has on ground motions from moderate earthquakes. The Pt. Mugu (M 5.3) and Santa Barbara (M 5.8) earthquakes both result in greatly amplified ground motions in the central basin; in both cases, ground motions vary across the basin-bounding faults by up to 100%.

The deep basin allows the propagation of the ground motions of even smaller events (e.g. Santa Barbara, M5.8) much further than in the adjacent basin margins to the north and south. This is especially apparent for earthquakes that occur east or west of the basin, along the basin's axis. For instance, at the eastern extent of the basin, ground motions from the Santa Barbara earthquake have attenuated to 0.03-0.04g on the flanks of the basin, while within the basin PGA values of 0.07-0.08 g are present at equivalent distances from the earthquake.

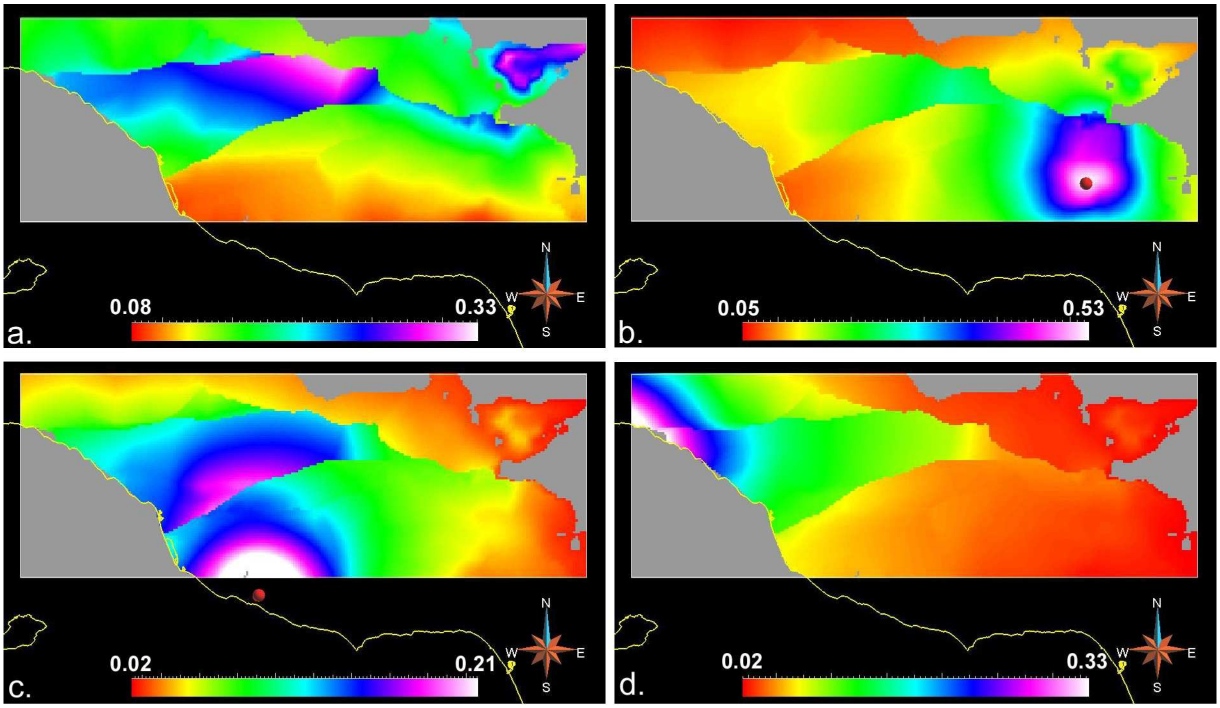

Figure 8. Calculated PGA values in the Ventura Basin for four historic earthquakes. a) 1857 Ft. Tejon (M7.9); b) 1994 Northridge (M 6.7); c) 1973 Pt. Mugu (M 5.3); and d) 1979 Santa Barbara (M 5.8). Gray areas represent regions of high velocity basement rock that were not included in the P-wave velocity model. Note the amplification effect of the deep central region of the Ventura basin for all cases. Note the different color scales for the four scenarios.

Because the primary effect of the basin geometry in this relation is the basin depth, the detailed velocity structure of the basin is not considered in these calculations. However, this attenuation relationship provides a first order illustration of the effect of basin geometry on coseismic ground motions, and the results clearly demonstrate the effect of basin depth on amplification of the ground motions. It should also be noted that these calculations did not consider dynamic effects such as rupture directivity or basin resonance. Such factors will be explored through future numerical ground motion models that incorporate the three-dimensional velocity model of the basin.

Conclusions

The structure and P-wave velocity in sedimentary basins distribution influence the effects of coseismic ground motions. We assessed these effects in the Ventura basin, a tectonically active basin containing a thick Cenozoic sedimentary section, by constructing a three-dimensional structural model of the basin using published maps and cross sections and petroleum industry well and seismic reflection data. The structural model of the basin incorporated the top Cretaceous surface, which represents a well defined transition in lithology and velocity structure, as well as representations of faults that bound the margin of the basin. Sonic logs from 60 petroleum wells and stacking velocities from a regional seismic reflection survey were used to parameterize the P-wave velocity structure of the basin sediments. The velocity gradient can be described by a simple power law function of depth. This gradient was used to populate a velocity model, which was then used to assess coseismic ground motions for four historical earthquakes using empirical attenuation relationships for southern California. The results of these calculations clearly demonstrate the effect of basin structure and sediment thickness on ground motions for both regional and local seismic events. The velocity model will be incorporated into future numerical wave propagation simulations to assess dynamic effects such as rupture directivity and basin resonance.

Bibliography

The results of this study will form a portion of the PhD dissertation of Charles Brankman, and will be submitted for publication in a peer-reviewed journal in the next several months.

References

Argus, D. F., Heflin, M. B., Donnellan, A., Webb, F ., Dong, D., Hurst, K. J., Jefferson, D. C., Lyzenga, G. A., Watkins, M. M., Zumberge, J. F., 2000, The velocity field in Southern California determined from the permanent GPS SCIGN array, Seismological Research Letters, vol.71, no.2, pp.254.

Corbett, E. J., and Johnson, C. E., 1982, The Santa Barbara, California, Earthquake of 13 August, 1978: Bulletin of the Seismological Society of America, v. 72, p. 2201-2226.

DeMets, C. Gordon, R. G., Stein, S., and Argus, D. F., 1987, A revised estimate of Pacific-North America motion and implications for western North America plate boundary zone tectonics: Geophysical Research Letters, v. 14, no. 9, p. 911- 914.

Donnellan, A., Hager, B. H., King, R. W., Herring, T. A., 1993 Geodetic measurement of deformation in the Ventura Basin region, Southern California, Journal of Geophysical Research, B, Solid Earth and Planets, vol.98, no.12, pp.21,727-21,739.

Graves, R.W., Pitarka, A., Somerville, P. G., 1998, Ground-motion amplification in the Santa Monica area; effects of shallow basin-edge structure, Bulletin of the Seismological Society of America, vol.88, no.5, pp.1224-1242.

Hager, B. H., Lyzenga, G. A., Donnellan, A., Dong, D.,, 1999, Reconciling rapid strain accumulation with deep seismogenic fault planes in the Ventura Basin, California, Journal of Geophysical Research, B, Solid Earth and Planets, vol.104, no.11, pp.25,207-25,219.

Hauksson, E., 1990, Earthquakes, faulting and stress in the Los Angeles Basin: Journal of Geophysical Research, v. 95, p. 15365-15394.

Huftile, G. J. and R. S. Yeats, 1995, Convergence rates across a displacement transfer zone in the western Transverse ranges, Ventura basin, California, *J. Geophys. Res.* 100, 2043-2067.

Kamerling, Marc J; Sorlien, Christopher C; Archuleta, Ralph; Nicholson, Craig, 2001, Three-dimensional geometry and interactions of faults and structures along the northern margin of the Santa Barbara Channel, California, AAPG Bulletin, vol.85, no.6, pp.1127-1128.

Larsen, S., Agnew, D. C., and Hager, B. H., 1993, Strain accumulation in the Santa Barbara Channel, 1970-1988: Journal of Geophysical Research, v. 98, no. B2, p. 2119-2133.

Larson, K. M., and Webb, F. H., 1992, Deformation in the Santa Barbara Channel from GPS measurements, 1987-1991: Geophysical Research Letters, v. 19, no. 14, p. 1491.

Mallet, J. L., Discrete smooth interpolation in geometric modeling, *Comput. Aided Design*, 24(4), 178–191, 1992.

Minster, J. B. and Jordan, T. H., 1978, Present-day plate motions: Journal of Geophysical Research 83, p. 5331-5354.

Mount, V. S., and Suppe, J., 1992, Present-day stress orientations adjacent to active strike-slip faults, California and Sumatra: Journal of Geophysical Research, v. 97, no. B8, p. 11,995-12,031.

Namson, J., and Davis, T. L., 1988a, A Structural transect of the western Transverse Ranges, California: Implications for lithospheric kinematics and seismic risk evaluation: Geology, v. 16, p. 675-679.

Plesch, A., J. H. Shaw, C. Benson, W. A. Bryant, S. Carena, M. Cooke, J. Dolan, G. Fuis, E. Gath, L. Grant, E. Hauksson, T. Jordan, M. Kamerling, M. Legg, S. Lindvall, H. Magistrale, C. Nicholson, N. Niemi, M. Oskin, S. Perry, G. Planansky, T. Rockwell, P. Shearer, C. Sorlien, M. P. Suess, J. Suppe, J. Treiman, and R. Yeats (2005), Community Fault Model (CFM) for Southern California, *BSSA*, in review.

Porcella, R.L., Etheredge, E.C., Maley, R.P., and Acosta, A.V., 1994, Accelerograms recorded at USGS National Strong-Motion Network stations during the Ms=6.6 Northridge, California earthquake of January 17, 1994, USGS Open File Report OFR 94-141, 102 pages.

Reed, R. D., and Hollister, J. S., 1936, Structural evolution of southern California: Tulsa, Oklahoma, American Association of Petroleum Geologists, 157 p. Satoh, T., H. Kawase, T. Sato, and A. Pitarka (2001). Three-dimensional finite-difference waveform modeling of strong motions observed in the Sendai basin, Japan, *Bulletin of the Seismological Society of America 91,* 365–380.

Scientists of the U.S. Geological Survey and the Southern California Earthquake Center (1994). The magnitude 6.7 Northridge, California, Earthquake of 17 January 1994, *Science* 266, 389–397.

Shaw, J. and J. Suppe, 1994, Active faulting and growth folding in the eastern Santa Barbara Channel, California, *Geological Society of America Bulletin*, 106/5, 607-626.

Süss, P., and J. H. Shaw, P wave seismic velocity structure derived from sonic logs and industry reflection data in the Los Angeles basin, California, *Journal of Geophysical Research 108*(B3), doi:10.1029/2001JB001628.

Vedder, J. G.; Wagner, H. C. and Schoellhamer, J. E., 1969, Geological framework of the Santa Barbara Channel region, *in* Geology, Petroleum Development and Seismicity of the Santa Barbara Channel Region, California: U. S. Geological Society Professional Paper 679-A, p.1-11.

Ventura, C.E., Finn, W.D.L., and Schuster, N.D., 1995, Seismic response of instrumented structures during the 1994 Northridge, California, earthquake, *Canadian Journal of Civil Engineering*, v.22, p. 316-337.

Yeats, R.S., 1977, High rates of vertical crustal movement near Ventura, California, Science, v. 196, p.295-298.

Yeats, R. S., 1983, Large-scale Quaternary detachments in Ventura basin, southern California: Journal of Geophysical Research, v. 88, no. B1, p. 569-583.

Yeats, R. S., 1988, Late Quaternary slip rate on the Oak Ridge fault, Transverse Ranges, California, Implications for seismic risk: Journal of Geophysical Research, v. 93, p. 12,137-12,159.

Yeats, R. S., Huftile, G. J., 1995, The oak Ridge fault system and the 1994 Northridge earthquake, Nature, 373, 418-420.

Yeats, R. S., Huftile, G. J., and Grigsby, F. B., 1988, Oak Ridge fault, Ventura fold belt, and the Sisar decollement, Ventura basin, California: Geology, v. 16, p. 1113-1116.

Zoback, M. D., Zoback, M. L., Mount, V. S., Suppe, J., Eaton, J. P., Healy, J. H., Oppenheimer, D., Rosenberg, P., Jones, L., Raleigh, C. B., Wong, I. G., Scotti, O., and Wentworth, C., 1987, New evidence on the state of stress of the San Andreas fault system: Science, v. 238, p. 1115-1112.